ME5304 Laboratory Section Report:

Flow over a Circular Cylinder in Wind Tunnel Test

Student

WEI HUANXIA A0285164Y

E-mail: huanxia.wei@u.nus.edu

Supervisor

Dr Yongdong CUI

04 Nov 2023

Department of Mechanical Engineering

CDE, National University of Singapore

Abstract

The flow over a circular cylinder is a classic problem in fluid mechanics, describing the fluid flow phenomena when a fluid moves around a fixed cylindrical object. This problem is of significant importance in real-world engineering scenarios, as structures like wind turbines, bridges, skyscrapers, cars, and airplanes might encounter flow characteristics related to this issue. In this report, a series of wind tunnel tests were conducted to investigate the phenomenon of flow over a circular cylinder with the help of hot wire probe, constant temperature anemometry (CTA), and Labview. The experimental setups, including hardware, calibration, test, were introduced in this report. Afterwards, the post-processing of the data, which is provided by Prof. Cui, related to turbulence was introduced and discussed. Drawing from our analysis, it becomes evident that, in this flow over a circular cylinder case, with the assistance of the aforementioned research methods, the shedding frequency of the Karman vortex street is approximately 250Hz. Matlab code by the author of this ME5304 report has been open-source distributed already.

1 Introduction

Wind tunnel is a kind of aerodynamic test facility, providing a fully defined and monitored aerodynamic environment, which is indispensable in fundamental fluids research and related industrial applications. In this report, a series of data post-processing of the low-speed wind tunnel test is conducted and described.

The case is the two-dimensional fluid, hereby is the air, flow over a circular cylinder. Despite the simplicity of the test conditions, a great deal of basic fluid mechanics theory is involved. Through this case, many researchers get valuable results and regularities. The features of the Karman vortices and the Strouhal number of vortex shedding (St) are always be noticed. In the one hand, some works focus on the low-Renolds-number and low-speed cases (Greco et al., 2020; Mironov et al., 2021; Ooi et al., 2020; Wang et al., 2018; Zhao, 2021), while in the other hand many others concentrate on the high-speed compressible conditions in suction-based wind tunnels (Chen et al., 2013; Jiang & Cheng, 2017).

When the fluid flows over the circular cylinder surface, the separation and transition will occur, which means the flow get away from the surface and forms a boundary layer, and the laminar flow transfers to turbulence, respectively. As for low Renolds number, the flow pattern shows its periodic semi-steady modal, which is known as von-Karman vortex shedding (street wake) (Chen et al., 2019). In this report, the features of vortex are to be processed and discussed.

The Strouhal number (St) is a dimensionless number describing oscillating flow mechanisms, which is important in aerodynamics (Strouhal, 1878). The Strouhal number is given in **Eq 1.**

$$St = \frac{fL}{V} \tag{1}$$

where: f is the frequency of vortex shedding or oscillation, L is the characteristic length (in this case, L is the diameter of the cylinder), and V is the velocity of the flow (hereby it is normalized to mean value). The details about Strouhal number and its applications will be discussed in the following text.

2 Experimental Setup

2.1 Device for Test

The experiment has been completed ahead of the student laboratory section. The experiments were conducted at the Temasek Laboratory at the National University of Singapore. The data was obtained in a low-speed open-loop close-jet wind tunnel, shown in **Fig 1a.** The design parameters of this wind tunnel are shown in **Tab 1.** The wind speed is provided by a blow-down motor, integrated before the inlet of the wind tunnel, which is controlled by a PWM controller. This wind tunnel has no diffusion section and the airflow is discharged directly into the room from the downstream side of test section.

Tab 1. *The specifications of low-speed wind tunnel in Temask Laboratory in NUS.*

Feature	Value
Motor	2.5kW, variable speed AC
Contraction Ratio	9.8:1
Test Section Dimension	L: 0.16 m, H: 0.16 m
Max. Flow Speed	33 m/s
Turbulence Level	0.25%

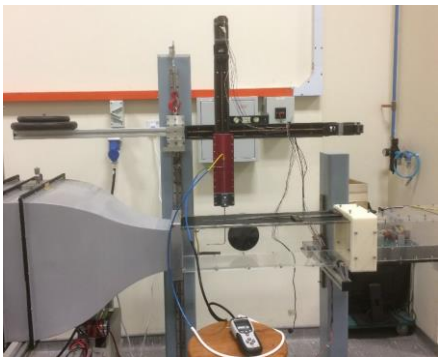

(a)

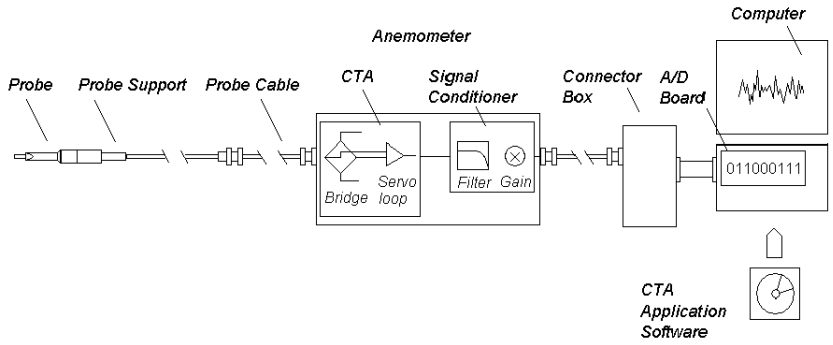

(b)

Fig 1. *Experimental setups.* **(a)** *the photo, and* **(b)** *the system connection schematic for the setup.*

A circular cylinder (d = 10 mm) was installed in the test section with end plate for two-dimentional tests. The wake of the cylinder is measured by a hot-wire probe, which goes through the wall of test section from the ceiling, and connected to a two-axis moving framework. The signal of probe is actively captured by CTA module, and then the voltage signal is converted to digital format in National Instruments data cquisition (DAQ) device. All cables in this setup are standard BNC coaxial cables. Labview tailor-made platform is installed on the computer for recording and preliminary analysis of flow field data. The system structure is shown in **Fig 1b.**

2.2 Power and Velocity

As the PWM controller of wind tunnel could only be controlled by power percentage, the generated wind speed is supposed to be calibrated. This means that the controllers are individually set to different power percentage levels and then the Pitot tube obtains the corresponding wind speed for the test section from downstream side. Accordingly, a mapping between controller settings and wind speed can be established, and basically linear, as shown in **Fig 2.**

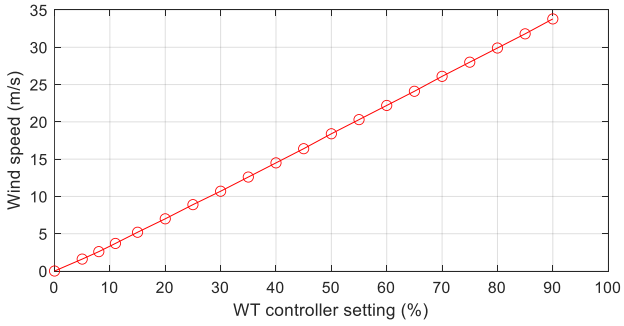

Fig 2. *Calibration mapping between wind tunnel controller setting and test section wind speed.*

2.3 Hot-Wire Calibration

Hot-wire anemometer probe is a sensor used to measure the velocity of fluid flow. The probe consists of a very thin wire, which is heated up to certain temperature above that of the fluid. As fluid flows over the wire, it cools the wire down, and the rate of cooling is proportional to the speed of the fluid flow.

The probe has an electrical resistance that changes with temperature. By measuring the resistance of the wire, the instrument can determine how much it has cooled, and thus the speed of the fluid flow.

However, the relationships between voltage (output signal) and velocity is influenced by external factors like temperature and setup. It was calibrated in order to obtain the relationship between the output voltage and the measured wind tunnel under the operating conditions of this test. The empirical formula suggests that, the relationship between voltage and velocity can be nearly obtained by Eq 2, which is also called “King’s Law”,

$$E^2 = aV^n + b \tag{2}$$

where a and b are fitting results, and n is normally near 0.5. Hereby n = 0.5 and n = 0.45 were attempted, and n = 0.5 shows a better fitting performance. By fitting under this case, the relationship is given by Eq 3, in which a and b become constant values.

$$E^2 = 0.718518\ V^n + 2.02978 \tag{3}$$

From this fitting, it could be easily known that the relationship between E^2 and $V^{0.5}$ is linear, and shown in **Fig 3a**. To validate the original fitting quality between E and V, the raw data and fitted curves are shown in **Fig 3b**, from which we can conclude the accuracy of this fit to be satisfactory.

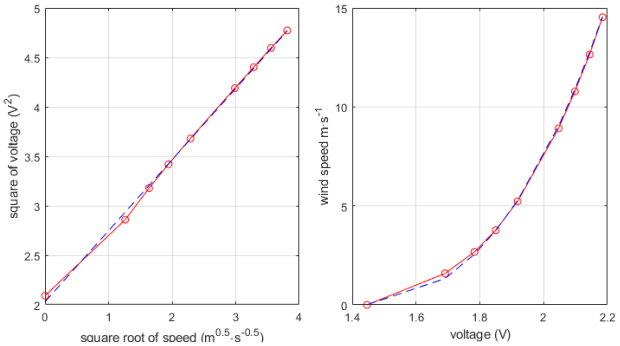

(a) (b)

Fig 3. *Hot-wire calibration results,* **(a)** *linear curve fitting with king's law (n=0.5), and* **(b)** *re-validation of data obtained from the fitting. Blue lines shows the fitting results as red ones are raw data. Residual Sum of Squares (RSS) is 0.123119, proving the fitting performance.*

This function provides the ability of mapping from the voltage to velocity in the following analysis.

3 Results and Discussion

3.1 Velocity and Time Domain

The raw data includes three different sampling frequency: 300Hz, 390Hz, and 6000Hz. If not being noted, the discribed data is 6000Hz, and the reason to choose it will be discussed in the next section.

Basic characteristics. Some basic turbulence-related parameters are calculated. The mean velocity of testing point is given by **Eq 4**, while the velocity fluction component $\widetilde{U}_I$ is the diffence between total velocity U and its mean value. The turbulence intensity In is given by **Eq 5-6**.

$$\overline{U} = \frac{1}{N}\sum_{i=1}^{N} U_i \tag{4}$$

$$\sigma = \sqrt{\frac{1}{N\text{-}1}\sum_{i=1}^{N} \widetilde{U}_i^{\,2}} \tag{5}$$

$$In = \frac{\sigma}{\overline{U}} \tag{6}$$

Afterwards, **Eq 7-8** shows the calculation of Skewness and Kurtosis of the flow signal.

$$S = \sum_{i=1}^{N} \frac{\widetilde{U}_i^{\,3}}{N\sigma^3} \tag{7}$$

$$K = \sum_{i=1}^{N} \frac{\widetilde{U}_i^{\,4}}{N\sigma^4} \tag{8}$$

Turbulence length scale is also an important turbulence characterizing parameter, obtained from the diameter of energy-containing eddy. The definition equation is **Eq 9**.

$$L_U = \frac{1}{\sigma^2}\int_0^{\infty} R_{p1,p2}(x)dx \tag{9}$$

However, it is obvious that in this eqution, data from multiple testing points (mininum two points: p1 and p2) are needed, and hereby only one point was monitored in this test. Nevertheless, Taylor's frozon hyperthesis (Taylor, 1938) could be used to solve this problem, thus which can be used to infer time dependencies from the spatial description of the turbulence. The hypothesis is based on the premise that, in a sufficiently high-speed turbulent flow, the fluctuation component of the fluid properties at a point can be considered to be "frozen" in time. Under this hypothesis, the turbulence length scale equation could be rewrited to **Eq 10**.

$$L_U^x = \frac{\overline{U}}{\sigma^2}\int_0^{\infty} R_{\widetilde{U}}(\tau)d\tau \tag{10}$$

This equation can be used for continuous, infinite-time signals. Based on our test, it could be dicretized to **Eq 11** (in which T means the windowed testing period, equal to (N-1)×dt, and dt is the time step which is 1.6667e-4 s here), and finally obtain **Eq 12**, in which all the variables are known or calculated already.

$$L_U^x = \frac{\overline{U}}{\sigma^2} \cdot \frac{\sum_{i=1}^{N} R_{\widetilde{U}_i}(\tau_i)}{N\text{-}1} \cdot T \tag{11}$$

$$L_U^x = \frac{\overline{U}\cdot dt}{\sigma^2}\sum_{i=1}^{N} R_{\widetilde{U}_i}(\tau_i) \tag{12}$$

Based on the equations and values (windowed to 0.01 second for length scale), the key parameters of test result as well as blank wind tunnel for reference are shown in **Tab 2**. It is worthy noting that the length scale is based on limited data on single point by Tarlor's hyperthesis, and might be biased.

Tab 2. *The key parameters of flow field of baseline and at the downstream wake of the circular cylinder.*

Parameter	Baseline	Cylinder
Mean velocity	12.763 m/s	12.147 m/s
RMS of velocity	0.0548 m/s	3.1590 m/s
Skewness	0.02278	-0.44829
Kurtosis	2.72329	2.96610
Turbulence intensity	0.4290 %	26.006 %
Turbublence length scale	19.142 mm	12.146 mm

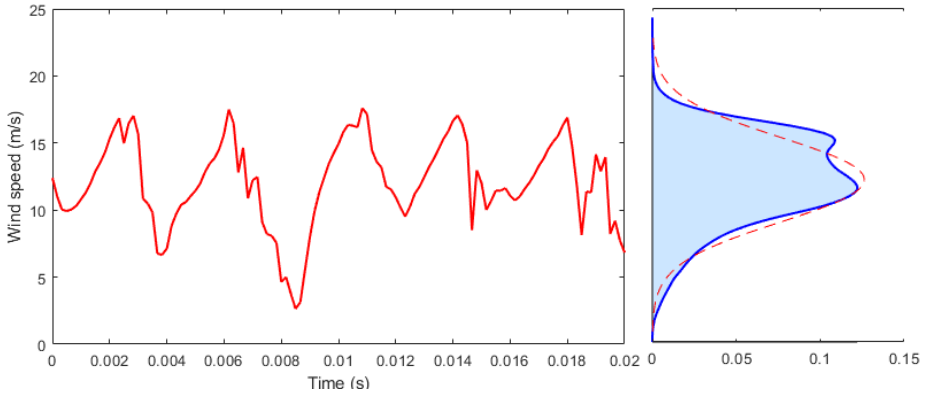

Fig 4. *The time domain signal of downstream velocity of circular cylinder and probability density function (PDF) with normal distribution fitting result. The time range is limited to first 0.02s, and the sampling frequency is 6000Hz. This data was captured at the point of x=25mm and y=5mm in the test section.*

Probability Density Function. Probablity indicates the distribution of velocity field, treated as time-averaged function, i.e., project the time axis toward the probability axis. In this case, the PDF was calculated under normal distribution, of which the definition is given by **Eq 13**, shown in **Fig 4**. together with the signal time domain (0.02s windowed).

$$f(x|\mu,\sigma)=\frac{1}{\sigma\sqrt{2\pi}}e^{-\frac{(x-\mu)^2}{2\sigma^2}} \quad (13)$$

Not surprisingly, the main peak appears slightly below the mean velocity, while a side peak is produced at upper side. The sidelobe density has decreased compared to the normal distribution.

Correlation Tests. This time domain analysis is to detect the correlation degree of the velocity data compared to itself after a certain delay. In this case, Pearson correlation (with "*corrcoef*") and Autocorrelation (with "*xcorr*") are conducted.

Pearson correlation coefficient is a linear correlation without normalization, i.e., the value will be affected by the amplitude. The calculation is given by **Eq 14**.

$$r_U = \frac{\sum(u_t-\overline{u_t})(u_{t+\tau}-\overline{u_{t+\tau}})}{\sqrt{\sum(u_t-\overline{u_t})^2\sum(u_{t+\tau}-\overline{u_{t+\tau}})^2}} \quad (14)$$

, in which r_U is Pearson correlation coefficient, τ is the time difference, and i is a randomized time step. From this equation, the static component would be ignored, which means u is the velocity fluctions (it is the same when it comes to other following ones).
In post-processing of wind tunnel tests, it aims to obtain the wake vortex shedding frequency. When the Pearson correlation coefficient returns to its first peak (exclude $\tau = 0$), the amount of change in the time sliding window (τ) is the vortex periodic. From the **Fig 5a**, the periodic is approximate 0.004s, revealing a shedding frequency of 250Hz.

Autocorrelation is a normalized correlation method, using mean velocity of the complete time domain instead of the one within the time sliding window of Pearson method. The definition is given by **Eq 15**, as the discrete and time-limited one is **Eq 16**.

$$R_U(\tau) = \lim_{T\to\infty}\frac{1}{T}\int_{-T/2}^{T/2}u(t)u(t+\tau)dt \quad (15)$$

$$R_U(\tau) = \frac{T}{N}\sum_{i=1}^{N}u(i)u(i+\frac{\tau}{dt}) \quad (16)$$

Autocorrelation figure (**Fig 5b**) could be applied for length scale calculation under Taylor's hyperthsis. The characteristic time is the time when the autocorrelation drops to zero, which in this sequence is 9.990e-4 second, indicating a Taylor's turbulence integral length scale of 10.46 mm.

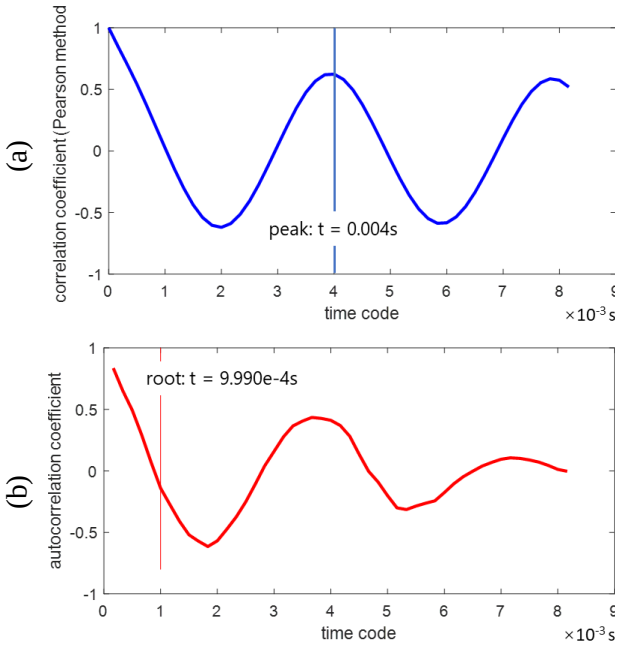

Fig 5. *Correlation tests of velocity time sequence,* **(a)** *the Pearson correlation test, and* **(b)** *the autocorrelation test.*

3.2 Frequency Domain

Frequency domain analysis is an important method in the fields of signal processing and data analysis, used to analyze the characteristics of a signal or data in the frequency domain (frequency space). Unlike time domain analysis, frequency domain analysis focuses on the properties and distribution of a signal's components at different frequencies, which helps us understand frequency features, periodicity, amplitude distribution, etc. In this report, Fast Fourier Transform (FFT) and Power Spectral Density (PSD) were applied to the wind tunnel velocity data.

Due to the results of frequency domain analysis, the reason of choosing 6000Hz as sampling freqency will also be discussed in this section.

FFT Spectrum. Fast Fourier Transform (FFT) is an indicator method for energy frequency distribution (dE vs f). It is a widely used mathematical algorithm for efficiently computing the Discrete Fourier Transform (DFT) of a signal or a sequence of data points, like velocity sequence here. The FFT spectrum is shown in **Fig 6a**.

PSD Spectrum. Power Spectral Density (PSD) is and indicator method for power frequency distribution (dP vs f).The significance of PSD mainly lies in the normalization of data at different sampling frequencies, which excludes the effect of sampling frequency on data analysis (this presupposes no frequency drift, i.e., the sampling frequency is more than twice above the frequency of interest, according to Shannon's Theorem). It could be calculated by **Eq 17** (interestingly, FFT is also included here).

$$S_x(f) = \lim_{Tw \to \infty} \frac{1}{Tw} |X(f)|^2 \qquad (17)$$

In this equation, X(f) is the FFT of time domain signal, and Tw is the size of time window function. Afterwards, to focus on the characteristics, a smoothing filter is added (shown in red line). The FFT spectrum is shown in **Fig 6b**.

Nyquist-Shannon's theorem is introduced here (Shannon, 1948), to describe the relationship between sampling frequency and signal frequency. When this sampling freqency is lower than twice of focused signal frequency, it would caused a down-scaled bias, which means the peak will appear at a lower frequency from the spectra. Obviously, both FFT and PSD shows a strong bias when sampled at 300Hz and 390Hz. What's more, 6000Hz is much higher than twice of peak (~500Hz) therefore acceptable while test. Finally, the estimated shedding frequency of the wake vortex is 255 Hz.

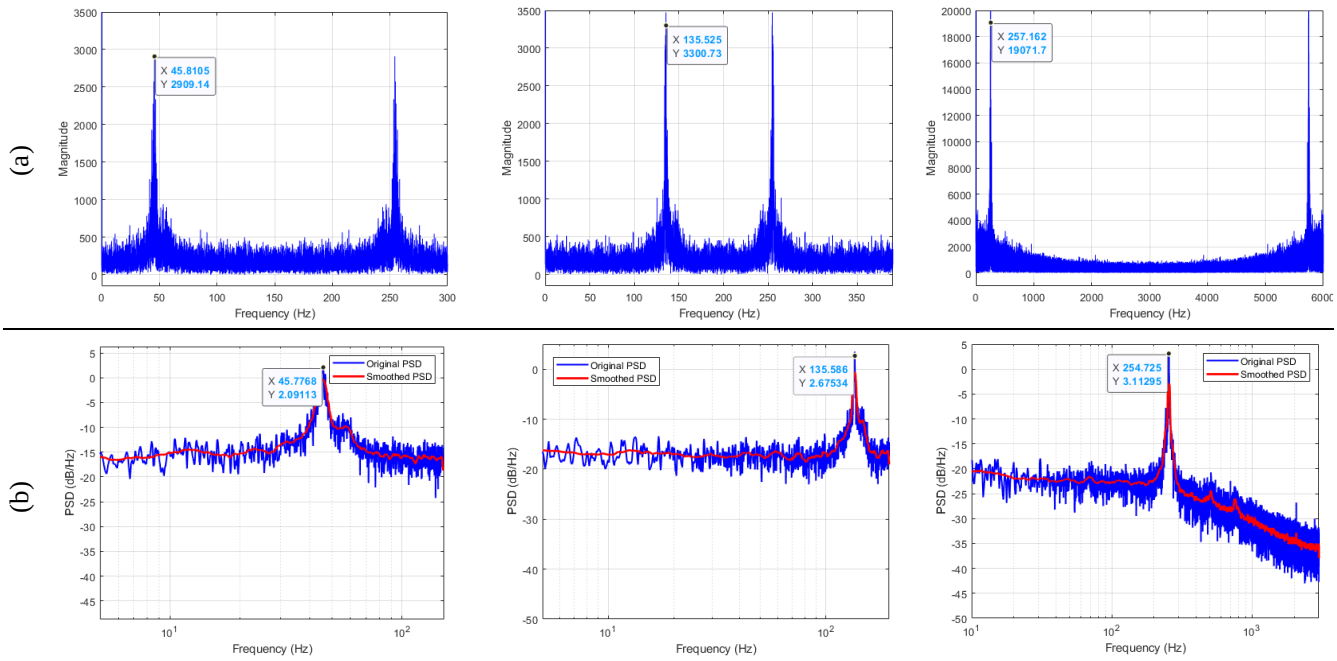

Fig 6. *Frequency domain analysis,* **(a)** *the FFT spectrum, and* **(b)** *the PSD spectrum of the velocity.*

3.3 Modal Decomposition

Variational Mode Decomposition (VMD) is a decomposition method for Intrinsic Mode Functions (IMFs) by matching the optimal center frequencies and finite bandwidths of the different modes, proposed by Dragomiretskiy at UCLA in 2014, and later extended to two dimensions (Dragomiretskiy & Zosso, 2015). The principle is to assume that all components are narrowband signals concentrated around their respective central frequencies, and accordingly build a constrained optimization problem to estimate the central frequency of each component. In this case, the modal number K seriously affects the effectiveness of the modal decomposition, and the optimal value of K can be obtained using the whale algorithm to reach the Optimal Variational Mode Decomposition (OVMD). Detailed equations will not be described here due to its high complexibility, which could take reference from citation (Dragomiretskiy & Zosso, 2014). The results are shown in **Fig 7**, while the respective power (normalized to percentage) and central frequency are shown in **Fig 8**.

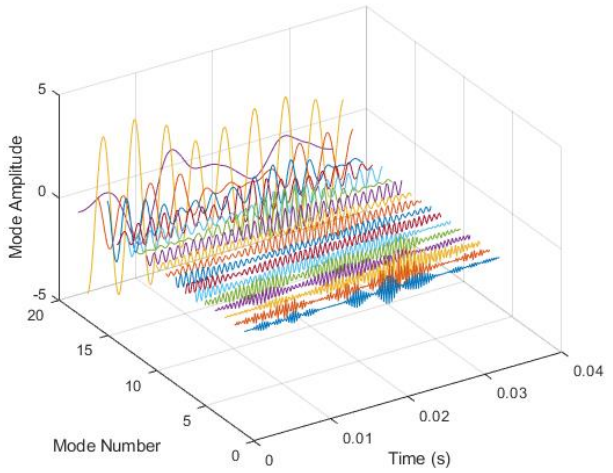

Fig 7. *The intrinsic mode functions by VMD. The steady modal is removed, and the total number of IMFs is 18.*

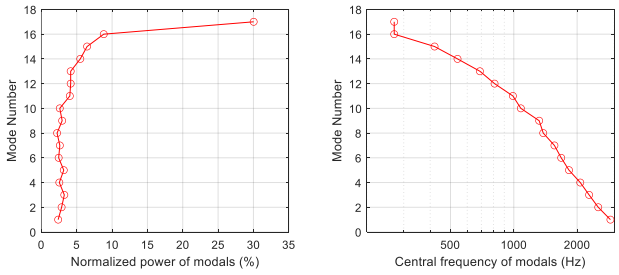

Fig 8. *The power percentage and central frequency of IMFs from VMD.*

Among all IMFs, the main fluction mode is #17, containing 30.04% power from total. Its frequency of peak in FFT is 270.0 Hz, only little higher than the shedding frequency of the wake vortex (255 Hz). From #16, the power suddenly drops to less than 10%. This indicates that the flow field is highly self-organized, and therefore it is in a quasi-steady state.

3.4 Errors Discussion

Firstly, the Renold's number can be easily calculated as 8221.04. From **Eq 1**, the Strouhal number of this case is 0.2099. Although, empirical relations show that under this case, the Strouhal number is approximately 0.205-0.210 (Achenbach & Heinecke, 1981), which means the results fits well.

Personally, in the one hand, the main error source is calibration of the hot-wire. As an empirical relation, Although King's law performs moderately well, it still has relative large. Additionally, temperature changes during the test will cause it to lose accuracy. In the other hand, the instability of the blowing-down turbine may also lead to errors. The turbulence intensity of a blank wind tunnel is 0.43%, which means it could still introduce turbulent components to the flow field of the test section, even though with very low turbulence level.

What's more, when the cylinder is mounted, it may vibrate or even displace slightly when facing high velocity airflow more than 10m/s, causing high Renold's number and chaos effect. This may also introduce unsatisfactory components to the signal.

4 Conclusions

In this report, a series of post-processing methods were applied for analysis of flow over a circular cylinder, especially focusing on the Karman vortex phenomenon and its shedding frequency. Before analysis, wind tunnel turbine calibration and hot-wire calibration were conducted, obtaining the relationships among the velocity, turbine power settings, and the voltage. For velocity and time-domain analysis, basic parameters were calculated while PDF and correlation tests were also obtained. For frequency domain, FFT and PSD were plotted, from the peak, the shedding frequency is estimated as 255 Hz, matching the theoretical value very well. Additinally, using VMD, the energy distribution and self-organization mechanism of the flow field were investigated in greater depth.

References

Achenbach, E., & Heinecke, E. (1981). On vortex shedding from smooth and rough cylinders in the range of Reynolds numbers 6e3 to 5e6. *Journal of Fluid Mechanics*, *109*, 239-251. doi: 10.1017/S002211208100102X

Chen, J. G., Zhou, Y., Antonia, R. A., & Zhou, T. M. (2019). The turbulent Kármán vortex. *Journal of Fluid Mechanics*, *871*, 92-112. doi: 10.1017/jfm.2019.296

Chen, W., Xin, D., Xu, F., Li, H., Ou, J., & Hu, H. (2013). Suppression of vortex-induced vibration of a circular cylinder using suction-based flow control. *Journal of Fluids and Structures*, *42*, 25-39. doi: 10.1016/j.jfluidstructs.2013.05.009

Dragomiretskiy, K., & Zosso, D. (2014). Variational Mode Decomposition. *IEEE Transactions on Signal Processing*, *62*(3), 531-544. doi: 10.1109/TSP.2013.2288675

Dragomiretskiy, K., & Zosso, D. (2015). Two-Dimensional Variational Mode Decomposition. Energy Minimization Methods in Computer Vision and Pattern Recognition,

Greco, C. S., Paolillo, G., Astarita, T., & Cardone, G. (2020). The von Kármán street behind a circular cylinder: flow control through synthetic jet placed at the rear stagnation point. *Journal of Fluid Mechanics*, *901*, A39, Article A39. doi: 10.1017/jfm.2020.427

Jiang, H., & Cheng, L. (2017). Strouhal–Reynolds number relationship for flow past a circular cylinder. *Journal of Fluid Mechanics*, *832*, 170-188. doi: 10.1017/jfm.2017.685

Mironov, D. S., Lebiga, V. A., Zinoviev, V. N., Pak, A. Y., Miau, J. J., Tsai, M.-C., & Lai, Y.-H. (2021). The features of 2D and 3D flow over circular cylinder with different surfaces. *AIP Conference Proceedings*, *2351*(1). doi: 10.1063/5.0052174

Ooi, A., Chan, L., Aljubaili, D., Mamon, C., Leontini, J. S., Skvortsov, A., Mathupriya, P., & Hasini, H. (2020). Some new characteristics of the confined flow over circular cylinders at low reynolds numbers. *International Journal of Heat and Fluid Flow*, *86*, 108741. doi: 10.1016/j.ijheatfluidflow.2020.108741

Shannon, C. E. (1948). A mathematical theory of communication. *The Bell System Technical Journal*, *27*(3), 379-423. doi: 10.1002/j.1538-7305.1948.tb01338.x

Strouhal, V. (1878). Ueber eine besondere Art der Tonerregung. *Annalen der Physik*, *241*(10), 216-251. doi: 10.1002/andp.18782411005

Taylor, G. I. (1938). The Spectrum of Turbulence. *Proceedings of the Royal Society of London. Series A - Mathematical and Physical Sciences*, *164*(919), 476-490. doi: 10.1098/rspa.1938.0032

Wang, S., Chen, Y., & Liu, Y. (2018). Measurement of unsteady flow structures in a low-speed wind tunnel using continuous wave laser-based TR-PIV: near wake behind a circular cylinder. *Journal of Visualization*, *21*(1), 73-93. doi: 10.1007/s12650-017-0445-3

Zhao, M. (2021). Flow past a circular cylinder and a downstream sphere for Re < 300. *Journal of Fluid Mechanics*, *913*, A20, Article A20. doi: 10.1017/jfm.2020.1123

Distribution

The MATLAB code to conduct post-processing and analysis will be made to open-source by the author, i.e., H.Wei from NUS. The distribution address is: https://github.com/hweifluids/wind-tunnel-toolkit-matlab currently. The source code is also included in the attachment together with this digital report.

More features will be introduced in the future 2023, potentially including: three-dimensional post-processing (incl. turbulence intensity, length scale, etc. This part is finished and will soon be released), turbulence integral length scale calculation with multiple points data (not based on Taylor's frozen hyperthesis as this report), boundary layer capture (gradient method and dissipation method), wind tunnel performance evaluation (based on multiple round-trip testing).